INTER-NOISE 2006
3-6 DECEMBER 2006
HONOLULU, HAWAII, USA

Calibrated modelling of low-frequency vibration in light weight timber floors

Colin Fox[a]
Mathematics Dept. & Acoustics Research Centre
The University of Auckland
PO Box 92019, Auckland
New Zealand

Hyuck Chung[b], George Dodd, Gian Schmid
Acoustics Research Centre
The University of Auckland
PO Box 92019, Auckland
New Zealand

Grant Emms
Scion Research
Te Papa Tipi Innovation Park
49 Sala St, Private Bag 3020, Rotorua
New Zealand

Ken McGunnigle
34 Barrys Point Road
Box 33-700 Takapuna, Auckland
New Zealand

ABSTRACT

A recent project completed at the Acoustics Research Centre succeeded in producing a cost-effective and buildable timber-framed inter-tenancy floor with impact sound insulation performance at least as good as a concrete slab. Typical light weight timber floor/ceiling structures consist of horizontal joists supporting an upper floor and lower ceiling, often via resilient rails, with damping material within cavities or as part of the flooring layer. The focus of that project was on low-frequency performance since the majority of noise complaints in relevant circumstances relate to intrusion of low frequencies. We present the modelling component of that work, and the calibration by test measurements. The use of an intuitively accessible variational model provided insight to the role played by components in traditional constructions and allowed subsequent design optimization. Within the model, representation of a composite structure is performed within the computational step, giving efficient computer implementation while maintaining flexibility to represent complex constructions. In particular the boundary conditions of individual building elements may be included in a simple way, which is an important consideration when modelling “flanking” paths for sound transmission.

1 INTRODUCTION

Buildings in New Zealand predominantly employ lightweight timber framed (LTF) construction, since LTF buildings are quicker and cheaper to construct than an equivalent in concrete. However, with LTF buildings there is a concern over poor sound insulation between neighbouring rooms that share a ceiling/floor or wall. Most disturbing, as measured by the number of complaints to noise-regulating authorities, is the low frequency ‘thumping’ noise generated by footsteps and electronic sound systems. The aim of this study is to model and predict in detail the acoustic performance of timber floor/ceilings, in the low-frequency regime, to provide a design tool and intuition for producing new practical LTF building designs that optimize sound insulation.

Figure 1 shows a cutaway drawing of a typical floor employing timber joists. As can be seen, the floor is a composite of simple components. Apart from horizontal supporting joists, this floor includes an upper floor, a lower ceiling that is suspended from metal rails by vibration-isolating clips, and porous sound-absorbing material in the cavities formed between joists, floor, and ceiling. A range of connection methods are possible including nails, screws, and glue, and of particular interest is the ability to include the mechanical properties of these various connection methods in a simple and realistic way so that their influence may be determined.

[a]Email address: fox@math.auckland.ac.nz
[b]Email address: hyuck@math.auckland.ac.nz

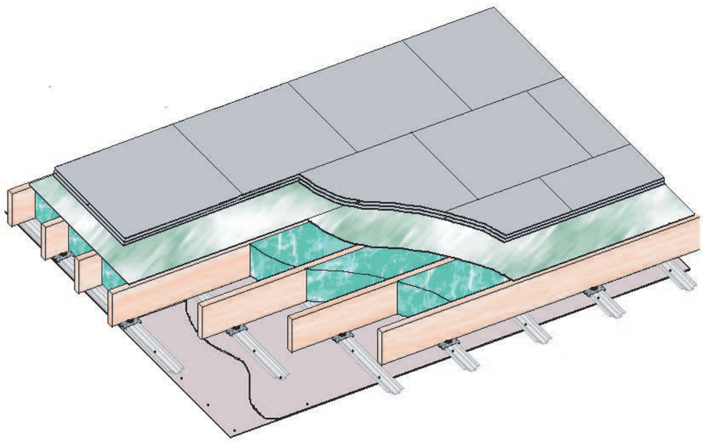

Figure 1: Cutaway schematic of a timber floor construction used in model calibration.

In our mathematical formulation we model the main components as plates (floor and ceiling) and beams (joists). We exploit the feature that the construction is layered and typically rectangular to construct the computational scheme.

The study reported here was adjunct to an industry and academic research consortium contracted by the (Australian) Forest and Wood Products Research and Development Corporation (FWPRDC) to design a timber floor with at least the sound isolation of a standard concrete floor.

2 MATHEMATICAL MODELLING

A series of articles by Hammer and Brunskog [1, 2] present detailed studies of the modelling of joist-floor vibration. Their technique is based on a model and solution developed by Mace [3, 4, 5] which assumes periodicity of the joist locations and a floor of infinite extent. These model the floor as a periodically stiffened thin plate, hence assume that components remain in contact though slip without resistance at the interface. That assumption seems dubious at best for actual timber floors. Infinite double leaf wall structures are studied in [6] and [7], also using Mace's solution, hence also assuming similar contact conditions.

Calculation of coupling loss factors for use in statistical energy analysis has lead to studies of vibration across a plate-beam connection [8, 9, 10] with more realistic contact conditions, using a method due to Ashton [11]. In [12, 13], these methods are used to find sound transmission through double-leaf walls with various contact conditions.

All these articles model vibration and sound transmission using differential equations derived using force-balance conditions. One difficulty of this approach is that *simplification* of the model is difficult since it requires comparison of vector forces which typically have large and small components within a single vector. In contrast, we adopt a variational formulation which is mathematically equivalent but has the substantial advantage of describing the dynamics in terms of scalar energies, which are directly comparable. A less obvious advantage of variational methods is that they are *closer* to consistent and efficient computational schemes, such as the finite element method and it's generalizations. In this section we derive the variational model and our computational scheme.

In addition to the existing theoretical models, Blazier and DuPree [14] suggested an empirical model based on homogeneous plate theory, which relates vibrational velocity to the impact sound pressure level (ISPL).

2.1 Variational Formulation

The variational formulation is based on the Lagrangian function [15]

$$\mathcal{L}\left(\mathbf{w}(t)\right) = \int_0^T \left[\mathcal{K}\left(t\right) + \mathcal{W}\left(t\right) - \mathcal{P}\left(t\right)\right] dt, \tag{1}$$

in which $\mathcal{P}$ and $\mathcal{K}$ are the instantaneous potential and kinetic energies of the structure, respectively, and $\mathcal{W}$ is the work done on structure by external forces. For a given motion $\mathbf{w}(t)$, the terms in the Lagrangian function may be calculated using the theory of linear elasticity [16]. The true motion of the structure $\mathbf{w}(t)$ makes the Lagrangian stationary with respect to *admissible displacements*. We use the restriction to admissible displacements to determine dominant modes of vibration by selective inclusion, in contrast to traditional numerical studies that base this on analysis of output from models allowing arbitrary motion.

For a single component (plate or beam) the *strain energy* is expressible as

$$\mathcal{P}(t) = \frac{1}{2}\int_V \epsilon_{ij}\tau_{ij} dx\, dy\, dz \tag{2}$$

(summation convention assumed) in which V is the volume occupied by the component, ϵ_{ij} and τ_{ij} are the strain and stress tensors, respectively. The kinetic energy is given by

$$K(t) = \frac{1}{2}\int_V \rho\|\dot{\mathbf{w}}\|^2 dx\, dy\, dz$$

in which $\dot{}$ denotes the time derivative, and ρ is the mass density per unit volume. For a homogeneous isotropic material the stress in equation 2 is a simple function of strain depending on the Young's modulus E and Poisson's ratio ν. We also assume a linear strain displacement relation since we are concerned only with small motions.

The classical plate and beam equations may be viewed as examples of modelling by selective inclusion of modes of vibration. For example, the classical Kirchhoff plate model follows from assuming that the middle surface S of the plate moves transversely, and that lines perpendicular to the middle surface remain perpendicular and unchanged in length. Then the motion of each point in the plate is a function of the transverse displacement of the middle surface, which we denote $w(x, y, t)$ for $(x, y) \in S$. In terms of that function, the strain energy is

$$\mathcal{P} = \frac{D}{2}\int_S \left(w_{xx}^2 + w_{yy}^2 + 2\nu w_{xx}w_{yy} + 2\left(1-\nu\right)w_{xy}^2\right)\, dxdy$$

while the kinetic energy is

$$\mathcal{K} = \frac{\rho h}{2}\int_S \left(\dot{w}^2 + \frac{h^2}{12}\|\nabla\dot{w}\|^2\right)\, dxdy$$

where $D = Eh^3/\left(12\left(1-\nu^2\right)\right)$ is the flexural rigidity and h is the plate thickness. Stationarity of the Lagrangian in equation 1, and neglecting rotational energy, gives the classical plate equation

$$D\nabla^4 w + m\ddot{w} = p\left(x, y, 0\right) \quad \text{in } S$$

where

$$\nabla^4 = \frac{\partial^4}{\partial x^4} + 2\frac{\partial^4}{\partial x^2 \partial y^2} + \frac{\partial^4}{\partial y^4}$$

is the biharmonic operator in the plane of the middle surface and $m = \rho h$ is the mass density per unit area.

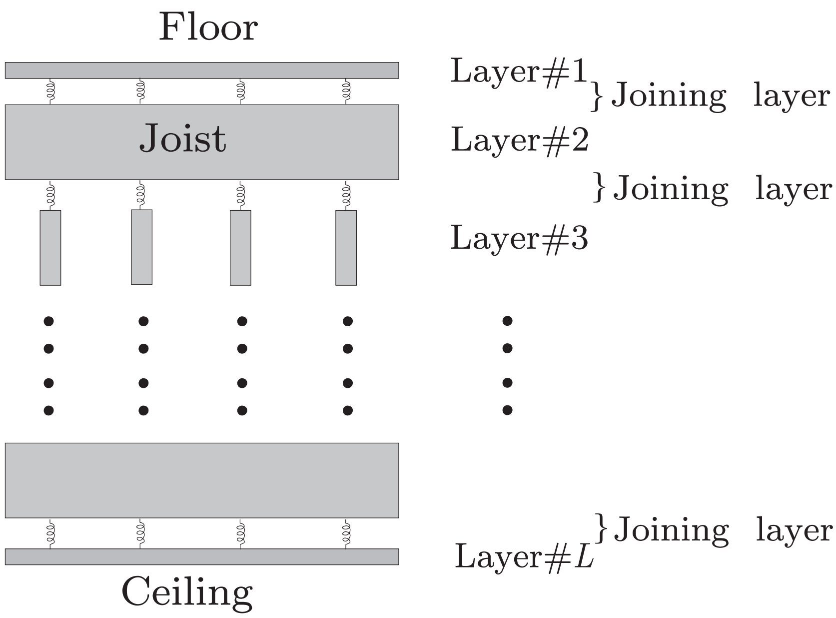

Figure 2: A layered structure showing components linked by springs that model the coupling.

2.2 Fourier Basis for a Single Component

Since we are concerned with small motion, and linear responses, we restrict time variation to $\exp\{i\omega t\}$ and appeal to superposition to calculate the response for arbitrary forcing. Then the time derivatives may be written as $\dot{} \equiv i\omega$.

We discretize the spatial representation of motion via a Fourier series as follows. For a plate with motion parameterized by the transverse displacement of the middle surface defined on the rectangle $(x, y) \in (0, A) \times (0, B)$ we write

$$w(x, y) = \sum_{m,n=0}^{N} c_{mn} \phi_m(x) \psi_n(y) \tag{3}$$

where

$$\phi_m(x) \propto \exp(k_m x) \quad \psi_n(y) \propto \exp(\kappa_n y) \quad \text{with} \quad k_m = \frac{\pi m}{A} \quad \kappa_n = \frac{\pi n}{B}.$$

These basis functions obey the convenient orthogonality relations $\langle \phi_n, \phi_m \rangle = \delta_{nm}$ and $\langle \psi_n, \psi_m \rangle = \delta_{nm}$. Also

$$\frac{\partial}{\partial x} \equiv k_m \quad \text{and} \quad \frac{\partial}{\partial y} \equiv \kappa_n.$$

Thus the differential terms become algebraic in each component, with discretization achieved by the finite summation in 3.

In this basis, the potential energy for the Kirchoff plate may be written as the quadratic form $\mathcal{P} = \frac{1}{2} c^{\mathrm{T}} M c$ where c is vector of coefficients $\{c_{mn}\}$, and M is the matrix $M = D\left(k^2 + \kappa^2\right)^2$ in which $k = \mathrm{diag}(k_{mn})$ and $\kappa = \mathrm{diag}(\kappa_{mn})$. Similarly, the kinetic energy is a quadratic form over the coefficients, c, and hence so is the Lagrangian. Finding a stationary solution is then easily found by solving the normal equations, or by directly minimizing the quadratic form.

2.3 Uncoupled Composite Structure

Figure 2 shows a cross section through a typical layered joist-floor construction. We exploit the layered structure to form a computational scheme for the composite structure. Motion of structural elements in layer l is parameterized by coefficients $c^l = \{c^l_{mn}\}$ for $l = 1, 2, \ldots, L$. For a plate layer the displacement is explicitly $w^l(x,y) = \sum_{m,n=0}^{N} c^l_{mn}\phi_m(x)\psi_n(y)$ while for a joist layer we write $w^l(x,n) = \sum_{m=0}^{N} c^l_{mn}\phi_m(x)$ for joist number $n = 1, 2, \ldots, N^l$. In each case, the potential energy for a component is the quadratic form $\mathcal{P}^l = \frac{1}{2}c^{l\mathrm{T}}M^l c^l$ for appropriate matrix M^l.

The potential energy of the structure, with no coupling between components, requires summing potential energies and work by force on the floor, to give

$$\mathcal{P} = \frac{1}{2}\begin{pmatrix} c^1 \\ c^2 \\ c^3 \\ \vdots \\ c^L \end{pmatrix}^{\mathrm{T}} \begin{bmatrix} M^1 & 0 & 0 & \cdots & 0 \\ 0 & M^2 & 0 & & \\ 0 & 0 & M^3 & & \\ & & & \ddots & \\ & & & & M^L \end{bmatrix} \begin{pmatrix} c^1 \\ c^2 \\ c^3 \\ \vdots \\ c^L \end{pmatrix} + \begin{pmatrix} f^1 \\ 0 \\ 0 \\ \vdots \\ 0 \end{pmatrix}^{\mathrm{T}} \begin{pmatrix} c^1 \\ c^2 \\ c^3 \\ \vdots \\ c^L \end{pmatrix}$$

or

$$\mathcal{P} = \frac{1}{2}c^{\mathrm{T}}Mc + f^{\mathrm{T}}c$$

for block matrix M.

2.4 Coupling and the Composite Model

Coupling between components in a composite structure is modelled by determining the *energy* associated with a (relative) motion of the components in question. This is relatively simple to do in terms of the local coordinates of each component. We restrict ourselves to energy functionals that are quadratic in the displacements of coupled components, and hence maintain the ease of solution that the uncoupled model has. Then the coupling force is equivalent to the restoring force of a spring with some spring constant. For this reason we depict the coupling forces in each mode of relative motion (transverse, slippage, rotation) by an appropriate spring.

Including coupling of this form then gives a block matrix system of the form

$$\mathcal{P} = \frac{1}{2}c^{\mathrm{T}} \begin{bmatrix} M^1 + J^{11} & J^{12} & J^{13} & \cdots & +J^{1L} \\ J^{21} & M^2 + J^{22} & J^{23} & & \\ J^{31} & J^{32} & M^3 + J^{33} & & \\ & & & \ddots & \\ J^{L1} & & & & M^L + J^{LL} \end{bmatrix} c + f^{\mathrm{T}}c$$

where J^{lm} represents the coupling between layers l and m (and is zero if there is no coupling). Again this is made stationary by solving the normal equations

$$M_{\mathrm{total}}c = -f$$

or directly minimizing the quadratic form.

We prefer the latter numerical method, using conjugate gradient optimization, since then we need only *operate* by the matrix M_{total} which is done by summing the operation of sub-matrices, and we do not need actually assemble M_{total}. In this way, we only need consider the energy for individual components, and the coupling energy between pairs of coupled components, and need never write equations for the whole structure.

2.5 Boundary Conditions and Flanking

Boundary conditions imposed by the mounting of the structure may be treated in two distinct ways. In our test rig the mounting was against a rigid masonry structure. Then the boundary conditions may be treated as a *constraint* on the allowable vector of coefficients c. For example, simply pinned mounting at the edge of the floor determines that the cosine terms in Equation 3 are zero, and one need only represent the sine terms. This potentially halves the number of coefficients. We do this in our simulations. However, more general mounting, such as when the floor is mounted in a timber-framed building, allow energy flow through the boundary of the floor and are better modelled by including the energy terms in the total Lagrangian.

These two approaches are actually mathematically equivalent, and interchangeable in theory. However the approaches lead to numerical problems with quite different stability, and the choice of which approach to use should be based solely on well-conditioning of the resulting normal equations.

3 MODEL CALIBRATION

3.1 Experimental Program

25 different configurations of floor/ceiling systems of the type shown in Figure 1 were tested. Each consisted of all, or some, of an upper plate, joist beams, sound absorbing glass-fibre, rubber clip, ceiling battens and ceiling panels, ranging from the simplest single layer upper plate and joist beams to multi-layer floor (including a layer of sand-sawdust mix) and multi-layer ceiling panels. Results in this section are presented for the floor depicted in Figure 1.

An electrodynamic shaker mounted on a beam straddling the floor was used to provide a vertical force on the floor upper surface. The shaker was connected to the floor through a wire stinger and force transducer. A scanning laser vibrometer (Polytec PSV 300) was used to measure the transverse velocity of the floor on a grid with a spatial resolution of 10-14cm. This gave a map of the surface velocity of the floor relative to the input force. The shaker was driven with pseudorandom signal with a energy from 10 to 500Hz, and a duration of 2 seconds, giving a frequency resolution of 0.5Hz in the calculation of spatial transfer function. We also measured input impedance of the floor via an accelerometer at the force transducer.

3.2 Stiffness of Ceiling Battens

In calibrating each model we fit many aspects and parameters of the physical model. At the outset of this study we were particularly interested in the effect of slippage between joists and floor on sound transmission – particulary since this effect is implicitly neglected in all existing models of vibration in rib or joist-stiffened floors. We found that correctly modelling slippage is essential in matching the *frequency* of the lowest resonances of the system, while assuming no slippage (as is most common) renders the model invalid since then the dominant physical motion is not represented and values of joist stiffness, etc, required to give a best-fit to data are far from the actual values.

Fitting of the stiffness of ceiling battens was another, unexpected, instructional phase of the model calibration. In that case the best fit parameters were far from manufacturers quoted values, however subsequent direct measurement showed that the best-fit model parameters were indeed the correct *dynamic* values, and these differed significantly from the elastic properties at static loading. Presumably this was a result of relaxation processes in the rubber used within the vibration isolating clips. That result, amongst others, gave us confidence that the variational model was correctly representing the major physical processes that contribute to sound transmission, at least in the low-frequency regime.

Figure 3 shows the predicted velocity amplitude for varying stiffness of the ceiling battens from 2500N/m to 33000N/m, along with the measured velocity amplitude. The predicted curves capture the *bumpy* feature in the experimental results near 100Hz when the stiffness is 11000N/m. This chosen stiffness value, 11000N/m, agrees with the calculated stiffness of the component from its dimension (cross section size). It is interesting that battens with the stiffness of about 5500N/m are also used by the building industry. Figure 3 clearly shows the difference between the stiffness 5500 and 11000.

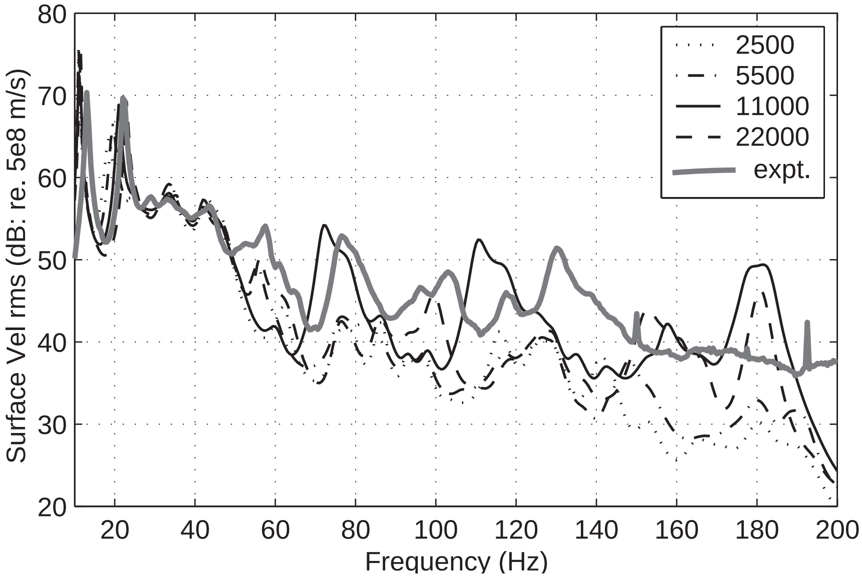

Figure 3: Predicted root mean square velocity of the ceiling surface for varying stiffness of the ceiling-battens, and measured values (expt.).

Figure 3 shows that the model fails to capture the peaks and the general shape of the measured curve for frequencies higher than about 100Hz, though the model predicts the approximate amplitude in that frequency range. We suspect one reason is that above 100Hz the assumption of line connection between the upper plate and the joist beams is no longer valid, as well as the assumption of a uniform single plate failing.

4 CONCLUDING REMARKS

We have presented a mathematical and computational model for low-frequency vibration of timber floors. The model is constructed by considering components separately, and in coupled pairs, with assembly of a total system of equations only in the computational step. Hence the model scales well with increased complexity of the floor construction.

Computation time required to 'solve' the model was small, allowing evaluation of designs using modest (standard desktop) computing requirements. This stems from the efficient discretization of the variational scheme using Fourier basis functions. In the low-frequency regime of interest, the model showed excellent fit to measured data with parameters accurately matching measured parameters. This gave confidence that the model actually described the main physical mechanisms in sound transmission., and allowed good predictive ability for the evaluation of new designs. That was essential in the overall success of the project to design a timber floor with performance in at least as good as a standard concrete floor.

The modelling work reported here was adjunct to the experimental program funded by the (Australian) Forest and Wood Products Research and Development Corporation (FWPRDC). A detailed report of all experiments, and further model calibration, will be available from the FWPRDC web site www.fwprdc.org.au/ at some future date.

5 REFERENCES

[1] P. Hammer, "Vibration isolation on light weight floor structures", Tech. Report TVBA-3078, Department of Engineering Acoustics, Lund University (1996).

[2] J. Brunskog, "Acoustic Excitation and Transmission of Lightweight Structures", PhD thesis, Lund University (2002).

[3] B.R. Mace, "Sound radiation from a plate reinforced by two sets of parallel stiffeners", Journal of Sound and Vibration, **71**, 435–441 (1980).

[4] B.R. Mace, "Periodically stiffened fluid-loaded plates, I: Response to convected harmonic pressure and free wave propagation", Journal of Sound and Vibration, **73**, 473–486 (1980).

[5] B.R. Mace, "Periodically stiffened fluid-loaded plate, II: Response to line and point forces", Journal of Sound and Vibration, **73**, 487–504 (1980).

[6] D. Takahashi, "Sound radiation from periodically connected double-plate structures", Journal of Sound and Vibration, **90**, 541–557 (1983).

[7] M. Yairi, K. Sakagami, E. Sakagami, M. Morimoto, A. Minemura, and K. Andow, *Sound radiation from a double-leaf elastic plate with a point force excitation: Effect of an interior panel on the structure-borne sound radiation*, Applied Acoustics, **63**, 737–757 (2002).

[8] R.S. Langley and K.H. Heron, "Elastic wave transmission through plate/beam junctions", Journal of Sound and Vibrations, **143**, 241–253 (1990).

[9] R.J.M. Craik and R. Wilson, "Sound transmission through parallel plates coupled along a line", Applied Acoustics, **49**, 353–372 (1996).

[10] R.J.M. Craik and R.S. Smith, "Sound transmission through lightweight parallel plate. part II: Structure-brone sound", Applied Acoustics, **61**, 247–269 (2000).

[11] J.E. Ashton and J.M. Whitney, "Theory of Laminated Plates", Technomic Publishing Co, Stamford, Conn. (1970).

[12] R.S. Langley, J.R.D. Smith, and F.J. Fahy, "Statistical energy analysis of periodically stiffened damped plate structures", J. Sound and Vibration, **208**, 407–426 (1997).

[13] R.J.M. Craik and R.S. Smith, "Sound transmission through double leaf lightweight partitions part I: Airborne sound", Applied Acoustics, **61**, 223–245 (2000).

[14] W.E. Blazier and R.B. DuPree, "Investigation of low-frequency footfall noise in wood-frame, multifamily building construction", J. Acoust. Soc. Am., **96**, 1521–1532 (1994).

[15] J. E. Lagnese, "Boundary Stabilization of Thin Plates", SIAM, (1989).

[16] I.H. Shames and C.L. Dym, "Energy and Finite Element Methods in Structural Mechanics", Taylor and Francis Publishers, (1991).